

# Corrosion fatigue crack initiation and growth in 18 Ni maraging steel

T. ALP\*

*King Abdulaziz University, Department of Chemical Engineering, Jeddah, Saudi Arabia*

Z. HUSAIN, R. A. COTTIS

*Corrosion and Protection Centre, University of Manchester Institute of Science and Technology, Manchester M60 1QD, UK*

Nucleation of fatigue cracks in air and 3.5 wt% NaCl solution has been studied in an 18 wt% Ni maraging steel. Specimens tested on reverse bending fatigue machine showed a marked decrease in fatigue strength of the steel in NaCl solution reducing the  $10^7$  cycles endurance limit from 410 MPa in air to 120 MPa. Microscopic studies revealed crack initiation to be predominantly associated with non-metallic silicate inclusions in both cases. In air, initiation is caused by decohesion of the inclusion/matrix interface, while in NaCl solution complete detachment of inclusions from the matrix results due to the dissolution of the interface. 70% more inclusions are quantitatively shown to be associated with cracks in NaCl solution than in air at the same stress levels. Experimental and theoretical  $S-N$  curves and inclusion cracking sensitivity data are consistent with the mechanism suggested. The final fracture occurs by the main crack consuming the inclusions ahead of it by the "unzipping" of the shear band produced between the crack tip and the inclusion ahead.

## Nomenclature

|                         |   |
|-------------------------|---|
| $I$                     | percentage of inclusions with associated cracks |
| $E_i$                   | elastic modulus of the inclusion                |
| $E_M$                   | elastic modulus of the matrix                   |
| $\sigma_{\text{local}}$ | local stress                                    |
| $\sigma_{\text{mean}}$  | net section stress                              |
| $N_i$                   | number of cycles to crack initiation            |
| $\Delta\epsilon_p$      | reversed plastic strain range                   |

## 1. Introduction

The 18 wt% nickel-maraging steels are strengthened by martensite transformation followed by precipitation hardening.

Maraging steels are classified as materials of ultra-high yield and tensile strengths, which are maintained at temperatures of at least 350°C. They are age hardened by a simple, relatively low-temperature maraging treatment at 450 to 500°C and subsequent air cooling. The ductile bcc nickel martensite in these materials is considerably less susceptible to cracking than the brittle, as-quenched martensite of conventional carbon steels, which are overhardened and much strained prior to tempering. Furthermore, maraging steels possess exceptionally high resistance to crack propagation, with  $K_{Ic}$  values up to  $180 \text{ MN m}^{-3/2}$ . Their high notched tensile strength ( $3100 \text{ MN m}^{-2}$ ) or resistance to fatigue does not depend on carbon, whose low content in these materials helps eliminate the risk of decarburization in processing.

For enhanced properties, the optimum structure of maraging steel should include an exceedingly fine array of  $\text{Ni}_3\text{Mo}$  precipitates less than 100 nm in size

and interparticle spacing; absence of segregation of foreign elements to prior austenite grain boundaries and interphase boundaries, accomplished by controlled purity and titanium and molybdenum additions; freedom from coarse platelets of  $\text{TiC}$  or  $\text{Ti}_2\text{S}$  or sigma.

The presence of flaws in a material will most certainly cause local stress concentrations and locally enhance cyclic plastic strain during fatigue loading [1] and influence the initiation and propagation of fatigue cracks. Large defects of the type formed during welding can bring about rapid initiation. Smaller faults, such as non-metallic inclusions, can generate likewise high local stresses and thus accelerate initiation of fatigue cracks. The crack initiation characteristics of inclusions are paramount in determining fatigue failures, surface inclusions being more harmful than subsurface ones. The size, shape, orientation, amount and type of inclusions bear important influence on fatigue characteristics [2].

Although considerable work has been carried out on the cracking of inclusions under alternating stresses on the one hand [3, 4] and on the behaviour of inclusions under corrosive conditions on the other [5, 6], data relating to the role of inclusions in corrosion fatigue is lacking. The present work is an investigation carried out into the fatigue crack initiation characteristics of a maraging steel in air and in aerated sodium chloride solution, particular emphasis being placed on the role of non-metallic inclusions in the initiation and growth of cracks in both environments. Although maraging steels have been reported by earlier workers to be very sensitive to non-metallic

\*Visiting Professor at UMIST, Department of Metallurgy, Manchester, UK.

TABLE I Composition

| Chemical composition | Fe    | Ni   | Co  | Mo  | Mn   | Si   | S     | P     | Cr   | Ti  | Nb   | C    |
|----------------------|-------|------|-----|-----|------|------|-------|-------|------|-----|------|------|
| (wt %)               | 72.35 | 17.3 | 7.7 | 1.5 | 0.08 | 0.03 | 0.008 | 0.013 | 0.25 | 0.5 | 0.05 | 0.16 |

inclusions [7], no tangible interpretation has been advanced as to the parts played by inclusions. Hence an attempt has been made in the present paper to shed some light on the influence of inclusions in reducing the fatigue strength of a maraging steel in corrosive environment.

## 2. Material and experimental procedure

The material studied in this investigation was a maraging steel designed to DTD specification 5212 with the chemical composition given in Table I.

The material was supplied in the form of a hot rolled bar in the solution treated condition. For solution treatment the material is heated at a temperature between 810 and 830°C for at least 30 min per 25 mm of section thickness. This homogenization treatment is followed by air cooling. Such a treatment yields the mechanical properties presented in Table II.

Flat specimens of the dimensions given in Fig. 1 were used with the longitudinal axis being along the rolling direction.

Fatigue tests were carried out using an Avery reversed bending fatigue machine with a cyclic frequency of 14 Hz and a capacity of 2.88 N m.

Tests were performed in laboratory air and in freshly prepared 3.5% aerated sodium chloride solution. The sodium chloride solution was brought into intimate contact with the specimen surface by means of a silicon rubber cell fitted over the specimen mounting points.

All specimens were examined metallographically before, during and after fatiguing to determine the crack initiation and growth processes. Optical observations were carried out by using Olympus and Reichart microscopes, while Philips and ISI DS130 transmission and scanning electron microscopes were used for high magnifications.

A Quantimet 720 was used in manual mode for the quantitative measurements of inclusions and the fatigue cracks associated with them.

## 3. Results

### 3.1. S-N curves

The results of applied stress amplitudes and number of cycles to failure obtained from 18 Ni Maraging steel subjected to fatigue tests in air and sodium chloride solution are presented in the form of *S-N* curves in Fig. 2. These results are in good agreement with findings relating to similar materials tested under similar conditions [8]; the corrosive environment reducing the stress amplitude required for a given fatigue life time in air. This effect is comparatively small for high

strain, low cycle tests, but it becomes significant for lower stresses and prolonged test durations. The  $10^7$  cycles endurance limit for the maraging steel in question diminished from about 410 MPa in air to 120 MPa in the corrosive medium.

### 3.2. Micrographs

The metallographic examination of the specimen surface and fracture surface was carried out using optical and electron microscopy. These investigations have revealed the fact that crack initiation in air as well as sodium chloride solution is almost exclusively associated with surface silicate inclusions of the form  $\text{FeO}_x \cdot \text{SiO}_2$ . Nevertheless, cracks associated with titanium-rich surface inclusions were occasionally encountered. Scanning electron microscopy was used to inspect the inclusions with cracks at high magnification. Fig. 3 reveals inclusions on the surface of fatigue specimens in air and the sodium chloride solution. It is clearly seen that while cracks initiate at the inclusions/matrix interface in air, a complete detachment of inclusion from the matrix by the dissolution of the interface occurs in the sodium chloride solution, where the crack seems to be starting at the equatorial point of the interface. The micrographs presented here depict the general pattern of events taking place in the vicinity of inclusions in both environments. A very close examination of an inclusion in a corrosion fatigued specimen (Fig. 4) at a very low stress clearly shows the dissolution of the interface between the inclusion (I) and the matrix (M) creating cavities. The inclusion itself has also been fractured with cracks (C) starting at the equatorial points of this angular inclusion.

### 3.3. Quantitative measurements

Preliminary examination suggested that specimens tested in a corrosive environment and removed after a certain percentage (e.g. 5%) of the expected life had a greater proportion of inclusions with associated

TABLE II Mechanical properties

| UTS (MPa) | 0.2% PS (MPa) | EL (%) | RA (%) | VHN |
|-----------|---------------|--------|--------|-----|
| 1000      | 930           | 16     | 81     | 325 |

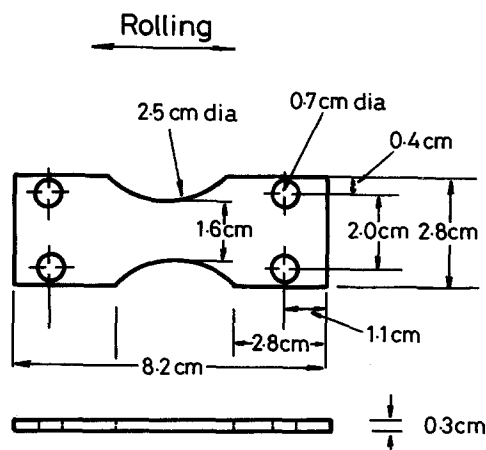


Figure 1 Test specimen.

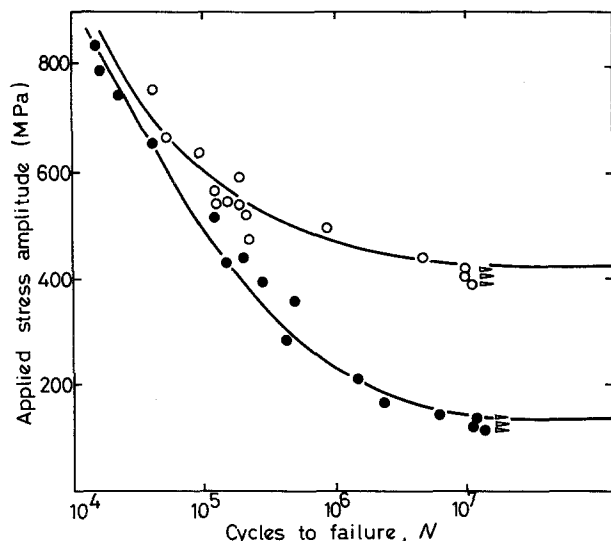


Figure 2 *S-N* curves for 18Ni maraging steel in air and 3.5 wt % NaCl solution. (O) air; (●) NaCl.

cracks than had specimens tested in air at the same stress level (even though the specimens tested in air would be exposed to a greater number of cycles, since their expected life was longer). Consequently some quantitative work has been accomplished using Quantimet in which the proportion of surface inclusions with an associated fatigue crack nucleus has been measured.

Fig. 5 illustrates the proportion of inclusions associated with cracks after 5% of expected life at a range of stress levels. It can be seen that for a given stress, tests in the corrosive environment yield about 70% more inclusions with cracks than tests performed in air. This quantitative approach was further extended to examine samples subjected to identical number of cycles at various stress levels. Even larger differences in %*I* were obtained between air and sodium chloride test results when the samples were fatigued at the same stress and for 2000 cycles, although the pattern of variation remained unaltered.

It is evident that with respect to stress as well as number of cycles, the plots for the sodium chloride solution are so displaced that the proportion of inclusions with crack (%*I*) is larger for the same conditions

of stress and number of fatigue cycles. This shows conclusively that the initiation and early growth of cracks is assisted by the chloride environment.

#### 4. Discussion

The evidence presented in Figs 2 to 5 unequivocally suggests that fatigue crack initiation in the maraging steel used in the present study is related almost exclusively to surface inclusions irrespective of the nature of the environment. This observation is further confirmed by the large proportions of inclusions found to have cracks associated with them after 5% of the expected fatigue life of the steel. The final fracture appears to result from a combined effect of microcracks initiated at individual inclusions whereby these microcracks eventually link and lead to catastrophic failure. This will be discussed shortly.

The generally accepted mechanism of crack initiation at inclusions involves debonding or decohesion of the inclusion/matrix interface [9]. In steels this interface is incoherent. Different elastic moduli of the matrix and inclusion give rise to elastic stress concentrations around particles which lead to local yielding. Hence, the stress on the interface rises progressively until decohesion occurs. This stage marks the formation of crack embryos which develop into larger cracks on subsequent deformation.

The occurrence of such a mechanism in the present case is supported by electron microscopic observations (Fig. 3). Furthermore, the fact that the proportion of inclusions allied to cracks falls as the stress amplitude is reduced is consistent with this mechanism. Since, at comparatively lower stresses fewer inclusions will build sufficiently large stress concentration to exceed the yield strength of the material, relatively fewer cracks could be generated.

This process can be modelled quite simply by assuming the stress concentration resulting from the inclusion to be a function of its geometry and linearly dependent on the ratio of the elastic moduli ( $E_i/E_m$ ) of the inclusion to that of the matrix. This leads to the relationship

$$\sigma_{\text{local}} = \sigma_{\text{mean}}[C(1 - E_i/E_m) + 1] \quad (1)$$

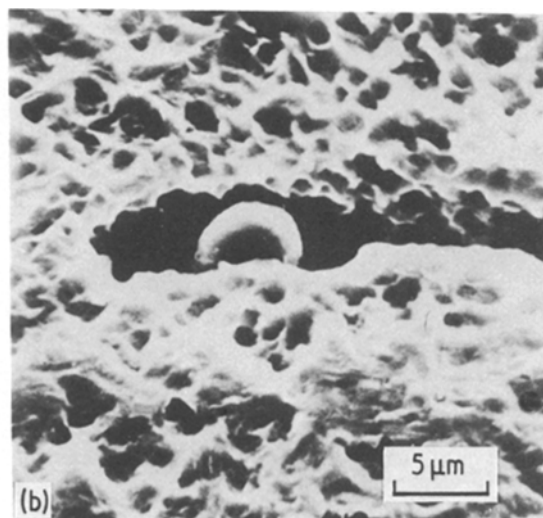
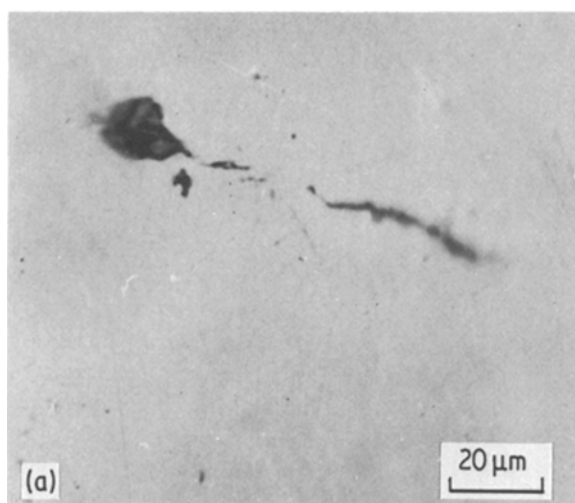


Figure 3 Microcracks associated with inclusions in (a) air, (b) NaCl solution.

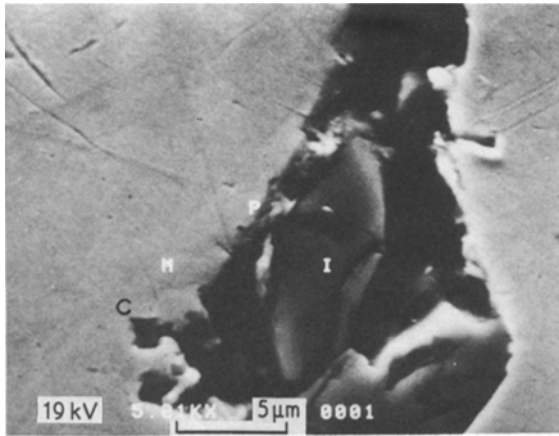


Figure 4 Dissolution of the interface between the inclusion (I) and matrix (M) leading to cavity formation. The inclusion also starts to crack at (c).

where  $\sigma_{\text{local}}$  and  $\sigma_{\text{mean}}$  are the local stress and net section stress, respectively.  $C$  is a geometrical constant. In a corrosive environment, a total dissolution of the interface results in a situation whereby the inclusion is detached completely from the metal leaving effectively a hole in the matrix. By using the above relationship with appropriate approximations it has been shown [10] that the stress concentrates by a factor of 2 in air, and by a factor of 4 in sodium chloride solution. Thus, corrosive decohesion of particles could potentially account for reducing the stress required to initiate a fatigue crack for a given number of cycles to half of the value required in air.

This analysis, however, applies to the crack initiation process only where a crack embryo is created by the debonding of the interface. The crack nucleation process may be considered to comprise initiation and microgrowth stages, the first of which is triggered by the stress concentration at the inclusion/matrix interface. Microgrowth of such an embryo then occurs under the stress concentration until the embryo attains a critical size at which it is capable of sustained growth at the applied stress intensity range. Such a nucleation process, would therefore, be affected by the variation in the critical size requirement ( $\Delta K_{\text{th}}$ ), the rate of

microgrowth and defect geometry, which influences the stress concentration and the plastic strain in the vicinity of the inclusions.

We now proceed to interpret the  $S-N$  curves of Fig. 2 in terms of the proposed model. It is well established that at high stress amplitudes crack initiation is facilitated irrespective of matrix uniformity, and crack propagation becomes the rate controlling factor. This will especially hold in the presence of inclusions because at high applied stresses, the local stresses and strains in the vicinity of inclusions become very large and initiation occurs with a corresponding ease. At the relatively high frequencies (14 Hz) used in the present tests crack propagation rates are expected to be essentially unaffected by the corrosive environment. Hence the propagation component of the failure time will be controlled by the stress amplitude, and will be the same for tests in air and sodium chloride solution. On the other hand, at lower applied stress amplitudes close to the fatigue limit in air, crack initiation constitutes the critical stage and the effect of corrosive environment on the nucleation of cracks bears its influence on the  $S-N$  curves so that the difference between the curves in air and sodium chloride environment assumes significance.

If an inclusion is large enough so that its debonding or cracking results in a defect larger than the critical size (above  $\Delta K_{\text{th}}$ ) then it is capable of growth thus eliminating the crack initiation stage. However, in the event of inclusions being below the critical size, a debonded inclusion crack will have to grow at slower rates under stress concentration before the stress intensity-controlled faster growth (above  $\Delta K_{\text{th}}$ ) takes over. In the present case the critical size was calculated to be about  $50 \mu\text{m}$ , which is larger than the largest inclusions present.

Hence, whether or not an inclusion is debonded does not alter the present analysis, because the increase in stress concentration in sodium chloride solution as derived earlier not only makes the debonding easier but also facilitates the growth of microcracks up to the critical size ( $\Delta K_{\text{th}}$  level). Hence, those small inclusions (bonded or debonded) associated with which no cracks could be observed in air, would reveal cracks in sodium chloride solution due to the effect of stress concentration on initiation and/or growth of microcracks. Therefore a larger proportion of inclusions would take part in generating cracks in sodium chloride solutions, as found in the present case (Fig. 5).

A distribution of sensitivities of inclusions to cracking can be determined with respect to the stressing conditions by plotting the available data of %I against the stressing condition based on Basquin's expression [11]. The stressing condition determined in terms of stress and number of cycles applied was  $\sigma^{1/6} N$  ( $1/6$  being the gradient of the  $\log \sigma$  against  $\log N$  curve) [11]. In sodium chloride solution the stress required to initiate the crack is reduced by a factor of two. Hence, the whole distribution should be displaced towards easier cracking in sodium chloride solution, corresponding to half the stress level required for air. A typical distribution of this kind is

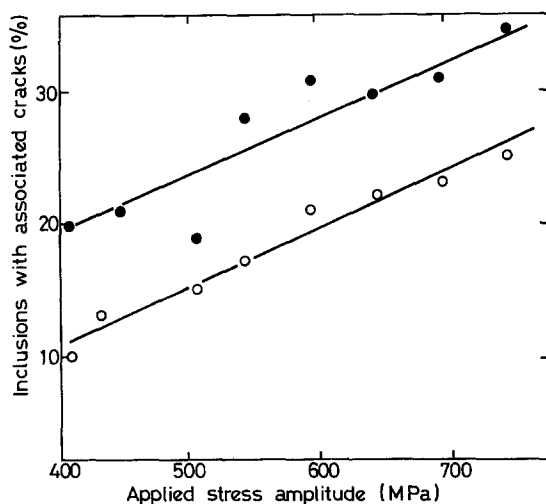


Figure 5 Proportion of inclusions with associated cracks as a function of stress. (O) air; (●) NaCl.

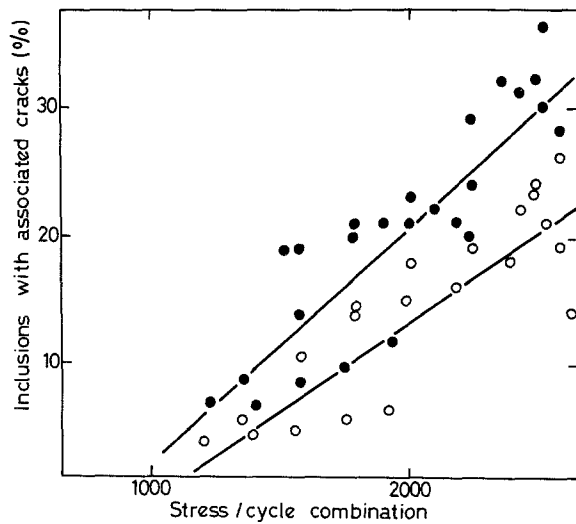


Figure 6 Distribution of sensitivity based on Basquins law [11]. Correlation coefficient: (○) air = 0.862; (●) NaCl = 0.858.

shown in Fig. 6 for the present case, and with remarkably high correlation coefficients of 0.862 (air) and 0.858 (NaCl solution). The distribution depicted in Fig. 6 is displaced, as expected, towards easier cracking.

The number of cycles to crack initiation ( $N_i$ ) is related to the reversed plastic strain range,  $\Delta\epsilon_p$  [1], which in turn is related to the stress concentration (and thereby to applied stress amplitude). Hence, theoretical  $S-N$  curves of applied stress against the number of cycles to crack initiation based on stress concentration at inclusions in air and sodium chloride solution can be plotted [11]. The similarity of these curves (Fig. 7) to experimental  $S-N$  curves further suggests that crack initiation at inclusions is indeed important in the present case. The large difference at high stresses compared to the experimental curves is due to the fact that these curves are solely based on crack initiation and the effect of growth is ignored.

In addition to low stress tests where initiation of cracks at inclusions is important, the significance of crack initiation is also reflected in the mechanism of fracture; that is whether the final fracture occurs by the conventional propagation of a crack initiated at an

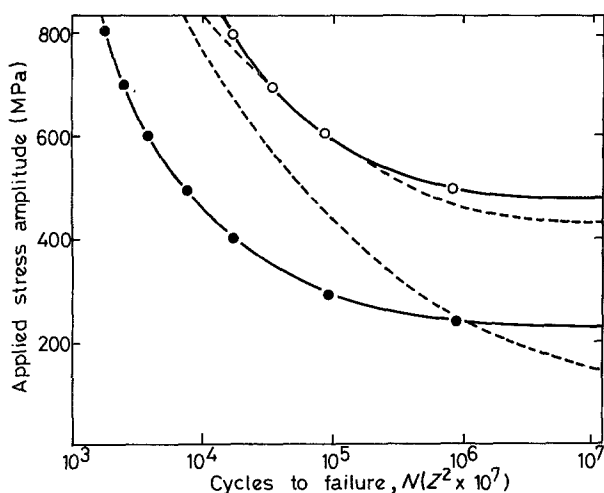


Figure 7 Theoretical  $S-N$  curves based on Coffin-Manson law. (○) air; (●) NaCl; (---) experimental curves.  $Z$  is a constant.



Figure 8 Cracks joining at inclusions. Arrows indicate inclusion locations.

inclusion or by a combination of cracks initiated at inclusions forming the crack advance path. In the latter case, the crack initiated at an inclusion advances and may join with a crack initiated at another inclusion on the crack propagation path.

The fact that crack advance occurred by the combinations of cracks at inclusions is substantiated by the type of observations such as that presented in Fig. 8, which shows the joining together of the inclusions. However, to study the phenomenon in more detail, a crack tip was observed at high magnification to look at the interaction between the inclusion and the advancing crack tip. Fig. 9a shows the microstructure of a plain specimen whereas Fig. 9b shows the specimen with a crack and an inclusion ahead of the crack tip. It can clearly be seen that a shearing of the material between the crack tip and the inclusion takes place. It seems possible that at a critical strain, this shear band “unzips” to advance the crack and consume the inclusion in a variant of the “unzipping” model of Chen and Knott [12].

## 5. Conclusions

1. Corrosion fatigue strength of the maraging steel was reduced so that the  $10^7$  cycles to failure endurance limit fell from 410 MPa in air to 120 MPa in sodium chloride solution.

2. Cracks initiate mainly at silicate inclusions. In sodium chloride solution stress concentration at inclusion doubles compared to air. This is attributed to “corrosive debonding”.

3. Corrosive debonding facilitates crack initiation as well as early growth of microcracks. Consequently more inclusions become associated with detectable cracks. More than 70% additional inclusions were observed to be associated with cracks in sodium chloride solution compared to air.

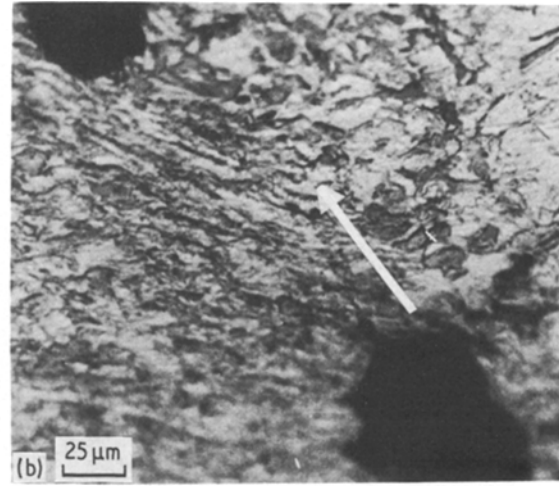
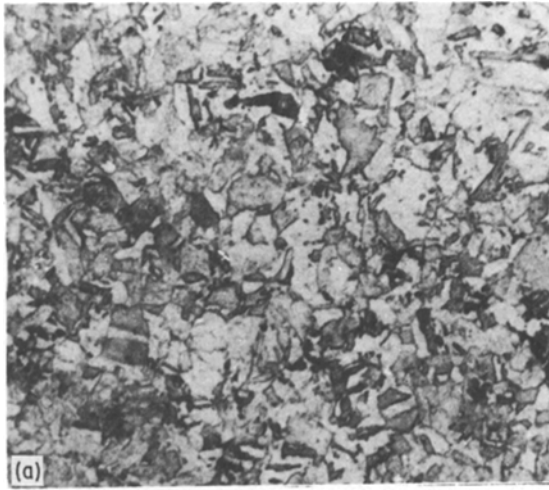


Figure 9 (a) Microstructure of the constrained specimen. (b) A crack tip and an inclusion ahead of it, with shearing taking place between them. The arrow shows direction of crack propagation.

4. Crack growth takes place by the linking together of cracks initiated at inclusions along the crack path. The main crack consumes inclusions by the “unzipping” of the shear band between itself and the inclusions ahead of it.

#### Acknowledgement

This research was carried out in the University of Manchester. The authors wish to thank Professor K. M. Entwistle of the Metallurgy Department and Dr R. Proctor of the Corrosion and Protection Centre for the provision of facilities. They also wish to thank Professor A. Argon of MIT and Mr D. Ryder of Hong Kong Polytechnic for their valuable suggestions.

#### References

1. G. HORKEGARD, *Eng. Frac. Mech.* **6** (1974) 795.
2. M. SUMITA, *Trans. Iron Steel Inst. Jpn.* **14** (1974) 275.
3. W. G. J. THROAT, *Nat. Aerospace Lab. (Netherlands)* **31** (1978) N79-17269.
4. J. LANKFORD and F. N. KUSENBERGER, *Metall. Trans.* **4** (1973) 553.
5. P. E. MANNING, *Corrosion* **36** (1980) 313.
6. V. SCOTTO, *Corr. Sci.* **19** (1979) 237.
7. P. JUBB, Iron and Steel Institute Special Report No. 76 (1962) 55.
8. W. STEVEN, Iron and Steel Institute Special Report No. 86 (1964) p. 115.
9. T. Y. SHIH and T. ARAKI, *Trans. Iron Steel Inst. Jpn.* **13** (1973) 11.
10. Z. HUSAIN and R. A. COTTIS, *Metals Technol.* **9** (1982) 104.
11. Z. HUSAIN, PhD thesis, UMIST, England (1982).
12. C. Q. CHEN and J. F. KNOTT, *Met. Sci.* **15** (1981) 357.

Received 30 August  
and accepted 21 November 1985